NUREG/CR-0037

RESIDUAL STRESSES AT WELD REPAIRS IN PRESSURE VESSELS

Quarterly Progress Report
September 1 - December 1, 1977

E. F. Rybicki R. B. Stonesifer

Battelle Columbus Laboratories

Prepared for

U. S. Nuclear Regulatory Commission

Available from
National Technical Information Service
Springfield, Virginia 22161
Price: Printed Copy $4.50 ; Microfiche $3.00

The price of this document for requesters outside of the North American Continent can be obtained from the National Technical Information Service.

NUREG/CR-0037
BMI-1994
R5

RESIDUAL STRESSES AT WELD REPAIRS IN PRESSURE VESSELS

Quarterly Progress Report
September 1 - December 1, 1977

E. F. Rybicki R. B. Stonesifer

Manuscript Completed: March 1978
Date Published: March 1978

Battelle Columbus Laboratories
505 King Avenue
Columbus, OH 43201

Prepared for
Division of Reactor Safety Research
Office of Nuclear Regulatory Research
U. S. Nuclear Regulatory Commission
Under Contract No. AT(49-24)-0293

TABLE OF CONTENTS

LIST OF TABLES

LIST OF FIGURES

I. INTRODUCTION

The introduction is organized to give the reader a summary of the first quarter's progress and to place this progress in perspective with the overall objectives. This is done through sections that summarize the objectives and the progress. The last section of the Introduction gives background information on the problem and the technical approach to accomplishing the objectives.

Objectives of the Study

The study is divided into three tasks. Task I is concerned with the residual stress distributions due to a weld repair of a pressure vessel. Task II examines the residual stresses due to an electron beam weld. Task III addresses the problem of residual stresses produced by weld cladding at a nozzle vessel intersection. The progress reported here is concerned with Task I; residual stresses due to a weld repair of a pressure vessel. The objective of Task I is to develop a computational model for predicting residual stress states due to a weld repair of a pressure vessel. The model is being developed through modifications of an existing residual stress analysis capability developed by Rybicki, et. al. [1], for girth-butt welds of pipes and pressure vessels. Residual stress results obtained with this model have shown good correlation with data for girth-butt welds. Thus, the approach, based on the computational model for girth-butt welds, appears to provide a reasonable starting point for developing a model to represent the weld repair problem. In fact, residual stress results from a preliminary application of this model to the weld repair of the Heavy Section Steel Technology Intermediate Test Vessel Number 8 (HSST ITV-8) have shown qualitative agreement with the residual stress data.

Summary Of Progress

During the first quarter, Task I efforts focussed on developing the temperature analysis model and the stress analysis model to represent the weld repair conditions of the HSST ITV-8 vessel. Progress has been made on developing the temperature analysis model to be applicable to the weld repair geometry. Based on selected test cases, computations were performed to study temperature

profiles and the effect of the vessel's inner surface on the temperatures. These studies showed that the simple heat flow model is an appropriate choice for the weld repair conditions.

The modifications of the stress analysis model to represent the weld repair geometry require substantially more development than those needed for the temperature model. Specifically, the weld repair is a relatively short axial weld with about 900 passes, while the girth-butt welds treated with the model were long circumferential welds with up to 30 passes. Thus, some three-dimensional effects must be developed in the stress analysis model. In addition, the weld repair is "buttered" with a half bead weld technique before the major welding is done. The effect of the buttering on residual stresses also needs to be examined.

Progress during this quarter included making changes in the stress analysis model to include (1) the additional stiffness due to the three-dimensional geometry, (2) plane strain effects, and (3) residual stresses due to the half bead weld technique. It was found that the three-dimensional stiffness effects of the weld repair geometry could be included in the existing two-dimensional model. This was verified by comparing stiffness and stress distribution characteristics obtained with the two-dimensional model with those calculated using a three-dimensional finite element analysis. Plane strain conditions were implemented in the computational model for temperature dependent elastic-plastic constitutive behavior and the capability was checked. Finally, a simplified model was developed to estimate the effect of the half bead weld technique on the residual stress distribution. The results of this model showed that the effect of the half bead weld procedure on residual stresses is not significant due to the depth of penetration of the temperature distributions.

Background and Approach

Welding is the most frequently used method of joining and repairing structural components of nuclear power plants. While welding provides many advantages over other joining techniques, the process introduces a complex distribution of residual stresses in and around the weld metal deposit. The magnitude and distribution of residual stresses are not easily determined. However, residual stresses can reach tensile values as high as the yield stress of the welded material. To alleviate the severity of residual stresses in weld

repairs and to produce a uniformity of weld repairs, a weld repair procedure has been adopted by the American Society of Mechanical Engineers [2]. However, the residual stress distributions due to this weld repair procedure are not well understood. New avenues for better understanding of weld induced residual stresses are being examined. Computational models have shown good correlation between predicted and measured residual stresses for certain weld geometries. However, the current state-of-understanding weld-induced residual stresses has not been developed to the point that the effects of weld parameters on residual stresses can be put in a handbook form.

The objective of the research reported on here is to examine the residual stresses near a weld repair in view of the recent developments in computational modeling for predicting weld-induced residual stresses [1]. A framework for such a study exists through the results of the Heavy Section Steel Technology (HSST) program [3]. Specifically, weld repairs have been conducted on intermediate sized test vessels and their prolongations* as part of the HSST program. Measurements have been taken on sectioned prolongations to estimate the residual stresses in the weld and the adjacent base material.

The study of weld repairs is divided into two parts. In the first part, a computational model is to be developed and evaluated based on the ability to predict residual stresses obtained from the weld repair region in the prolongation of the HSST ITV-8 vessel. The second part of the study involves a sensitivity study of some of the weld parameters to establish their effect on the final residual stress field. The purpose of the sensitivity study is to explore the possibility of reducing or redistributing residual stresses, by altering the weld repair procedure.

Efforts during the first quarter concentrated on the developmental aspects of the temperature and residual stress models. Technical progress is described in Sections II and III. Sections IV and V describe related activities and plans for next quarter, respectively.

---

* A prolongation is an open ended cylinder with the same thickness and diameter as the test vessel.

II. TEMPERATURE ANALYSIS MODEL

The geometric configuration for the weld repair is the eighth intermediate test vessel from the Heavy Section Steel Technology Program, designated HSST ITV-8. Figure 1 shows the geometry of the HSST ITV-8 weld repair cavity and the direction that the weld heat source travels. The temperature model being developed here is related to that used in the residual stress analysis for pipes and pressure vessels described by Rybicki et. al. [1]. The model gives the solution for a point heat source moving on the surface of a very large flat piece of material (i.e. a half space). The application of this type of model to the weld repair configuration is appropriate if for heat inputs and times of interest, the inner surface of the vessel and other geometric discontinuities do not affect the solution in the region of interest. Thus, this quarter's effort is not as concerned with developing the model as it is with checking its applicability for the various locations in the weld repair geometry. Also, of interest, is the fact that the model can be easily modified to represent the inside and outside corners shown in Figure 1. The remainder of this section contains the mathematical equations describing the temperature model, and the assumptions inherent to the model. Numerical examples selected to examine the limitations of the temperature model for the weld repair problem are contained in the Numerical Results part of this section.

The temperature in an insulated half-space due to the heat source moving on its surface is given by

$$T(r,\xi) = T_o + \frac{q}{2\pi Kr} \exp[-(\xi+r)Vc/K] \qquad (1)$$

where

T = temperature (F)

T_o = initial temperature

q = heat input (Btu/sec)

K = thermal conductivity (Btu/in-sec-F)

V = heat source velocity (in/sec)

ξ = distance from heat source to plane containing point of interest (in.)

r = distance from heat source to point of interest (in.)

c = heat capcity (Btu/in^3-F).

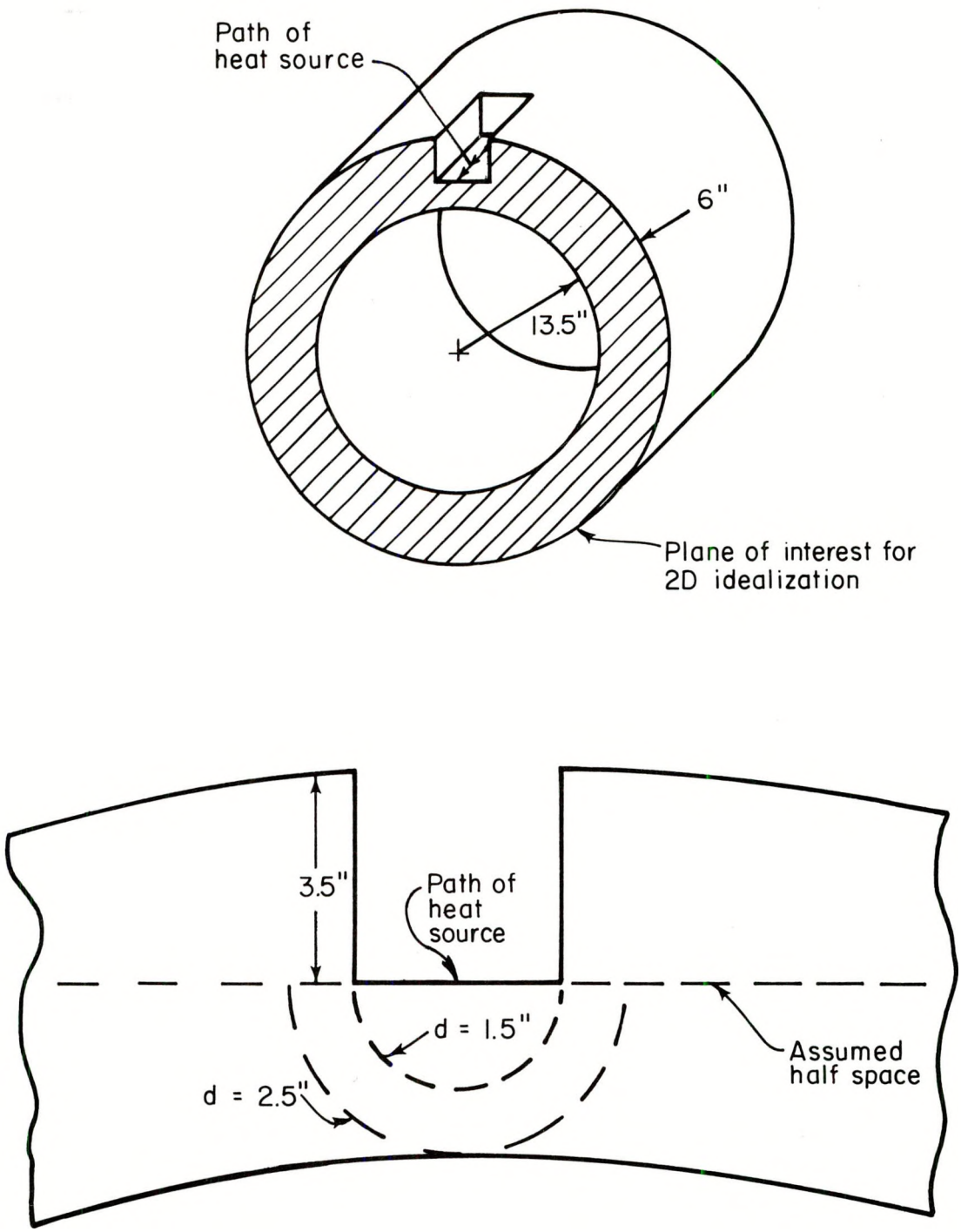

FIGURE 1. REPRESENTATIVE GEOMETRY OF THE WELD REPAIR FOR THE TEMPERATURE ANALYSIS OF THE HSST ITV-8 VESSEL

The steady distribution, described by Equation (1), moves with the velocity of the heat source. For this reason, time appears in the formula only implicitly through the equation $\xi = \xi_o - Vt$.

If Equation (1) is to be used without modification, then it is inherently assumed that the heat loss through the inner surface is not substantial enough to effect the final state of residual stresses. Two other assumptions are that (1) the welding process can be represented by a point heat souce moving on a straight line and (2) temperature dependent changes in the properties do not effect the temperature distributions at times of interest for residual stress calculations.

The formula stated in Equation (1) is valid for half space solutions. However, with only a slight modification, it can be used for solutions to quarter spaces or three-quarter spaces. These two cases are of interest in the weld repair analysis because a weld bead placed at the bottom of the weld cavity along one edge is essentially a three-quarter space problem and a buttering bead placed at the outer corner of the cavity is a quarter-space problem. The quarter-space solution is obtained by multiplying the second term in Equation (1) by two. The three-quarter space solution is obtained by multiplying the same term by two thirds. Thus, the effects of the corner locations shown in Figure 1 on the temperature history of the material can be obtained from the solutions provided by Equation (1).

Numerical Results

Numerical evaluations showed that even at low velocities and large rates of heat input, temperatures corresponding to the location of the pressure vessel inner surface are only slightly above the initial temperature during the time critical to residual stress. Thus, the assumption that the inner surface of the vessel has a negligible effect on temperatures near the heat source is justified for the geometry shown in Figure 1. Figure 1 also illustrates how the repair geometry generally corresponds to the basic assumption of a heat source moving on a large flat piece of material.

Other results were obtained in the form of the temperature history of several preselected locations within the vessel. As expected, the closer the point is to the heat source path, the higher and sharper the temperature peak becomes. For remote points, the peak is much lower and delayed relative to

the moment at which the heat source passes the point. For this initial study, welding parameters were selected to correspond to the 3/32-inch weld rod used in the buttering process. For this weld rod size, the average values used for the weld repair of the HSST ITV-8 vessel were given as 90 amps and 23 volts at a velocity of 7.5 inches per minute [3]. Figure 2 shows the time/temperature history for points at different locations in the plane of interest for this case. As previously mentioned, for times critical to residual stresses (less than 75 seconds for this arbitrarily chosen time scale) the vessel inner surface remains essentially at the initial temperature of 450 F and thus only a small modification of the model is needed to handle the repair geometry.

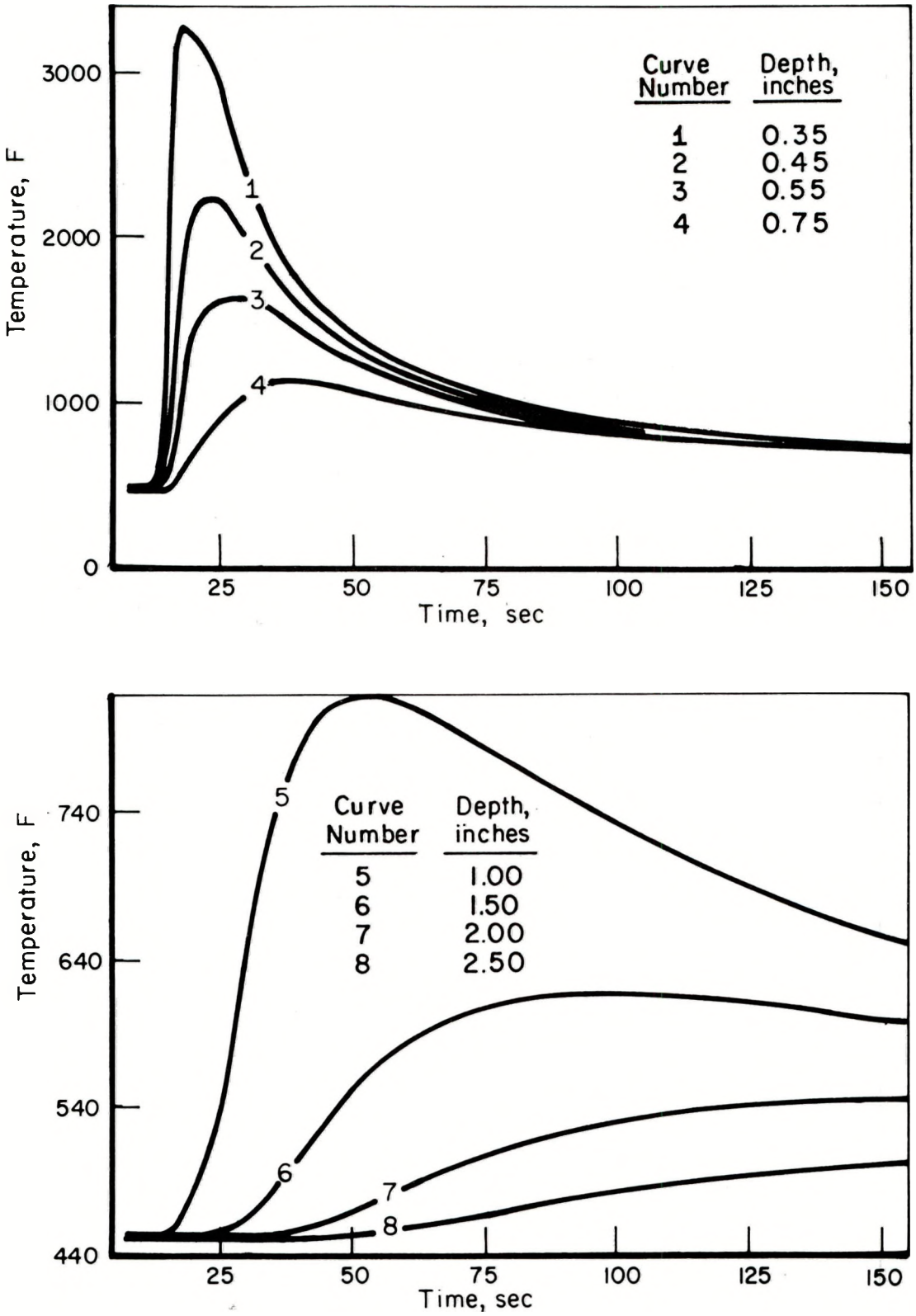

FIGURE 2. TEMPERATURE HISTORIES OF VARIOUS DEPTHS BELOW THE WELD TORCH

III. RESIDUAL STRESS ANALYSIS MODEL

The residual stress analysis model is based on a finite element representation of the weld repair region. The model includes representations of the weld geometry, the constitutive relations and the thermal loading. A cross section transverse to the weld direction is represented by a finite element grid. Each element is assigned to one of three zones. Zone 1 represents the weld material that is being deposited. Zone 2 is a region with essentially zero stiffness and is assigned to elements in areas to be filled by subsequent passes. Zone 3 consists of the base metal and the previously deposited weld material. The constitutive relations are incremental elastic-plastic equations based on the von Mises yield criterion and the Prandtl-Reuss equations. Temperature dependent properties for Young's Modulus, Poisson's ratio, yield stress and the strain hardening ratio are included in the constitutive relations. The constitutive relations can also represent elastic unloading from an elastic-plastic state of stress.

During each weld pass or each layer of weld passes being represented by the model, the thermal deformations and residual stresses are calculated based on temperature distributions determined by the temperature model. The residual deformations computed at the end of each pass or layer of passes are added to nodal point locations to determine an updated configuration of the model. Thus, the model represents large displacement, elastic-plastic problems as a series of incrementally linear problems using an updated lagrangian formulation.

The computer program uses quadrilateral elements, each composed of four constant strain triangles. This model has been used successfully by Rybicki, et.al. [1] for predicting residual stresses in girth-butt welds of pressure vessels and pipes. In addition, a preliminary calculation of residual stresses for a weld repair of the HSST ITV-8 vessel showed qualitative agreement with the residual stress data.

During the first quarter, modifications of the model were made in order to handle the three-dimensional and plane strain aspects of the weld repair geometry. These features and a simple model to study the effect of the half bead techniques on the residual stresses are described in the following.

Method for Including Three-Dimensional Stiffness Effects in a Two-Dimensional Model

The weld repair geometry is such that the two-dimensional (2D) assumption of plane strain could possibly have marginal justification. This is primarily due to the shortness of the repair in the axial direction as compared to the vessel wall thickness and weld repair width. In order to assess the applicability of the plane strain assumption, several three-dimensional (3D) elastic analyses were conducted for the ITV-8 geometry. The loading was selected so as to be self equilibriated in order to represent the type of loading imposed by a residual stress state. One load case consisted of uniform compression at the repair section and one of pure bending.

The 3D model of the HSST ITV-8 weld repair is shown in Figure 3. The axial length of the model is 21 inches and the axial length of the shaded load application region is 6.25 inches. Two sets of displacement conditions were imposed on the two load cases. In both solutions, symmetry boundary conditions were used at $y = 0$ and at $x = 0$ outside the loading region (see Figure 3). In addition, one solution was allowed no axial component of displacement at any section; this reinforced the plane strain aspect of the solution. For all the cases, an overall stiffness was determined by taking the ratio of the applied stress at the center of the weld and the corresponding displacement. Also, the variation in the σ_x components of stress at the outer surface was plotted as a function of angular position.

To determine the required stiffness to be added to the 2D model, a plane strain model of a cylinder was coupled to the plane strain model of the weld repair cross section. The concept upon which this method is based is that the portion of the model representing the cylinder can account for the stiffness of the ends of the vessel which do not contain the weld repair cavity. The method used to couple the two 2D models was simply to introduce linear springs between corresponding nodes of each model.

The 3D analysis with plane strain conditions permitted the effect of shear and bending deformation modes on the flexibility to be examined. It was found that the stiffness and overall stress state due to the bending type of applied loading was essentially unaffected by the addition of the plane strain constraint in the 3D analysis. The uniform stress loading on the outer hand showed a significant dependence on this type of axial constraint (plane strain).

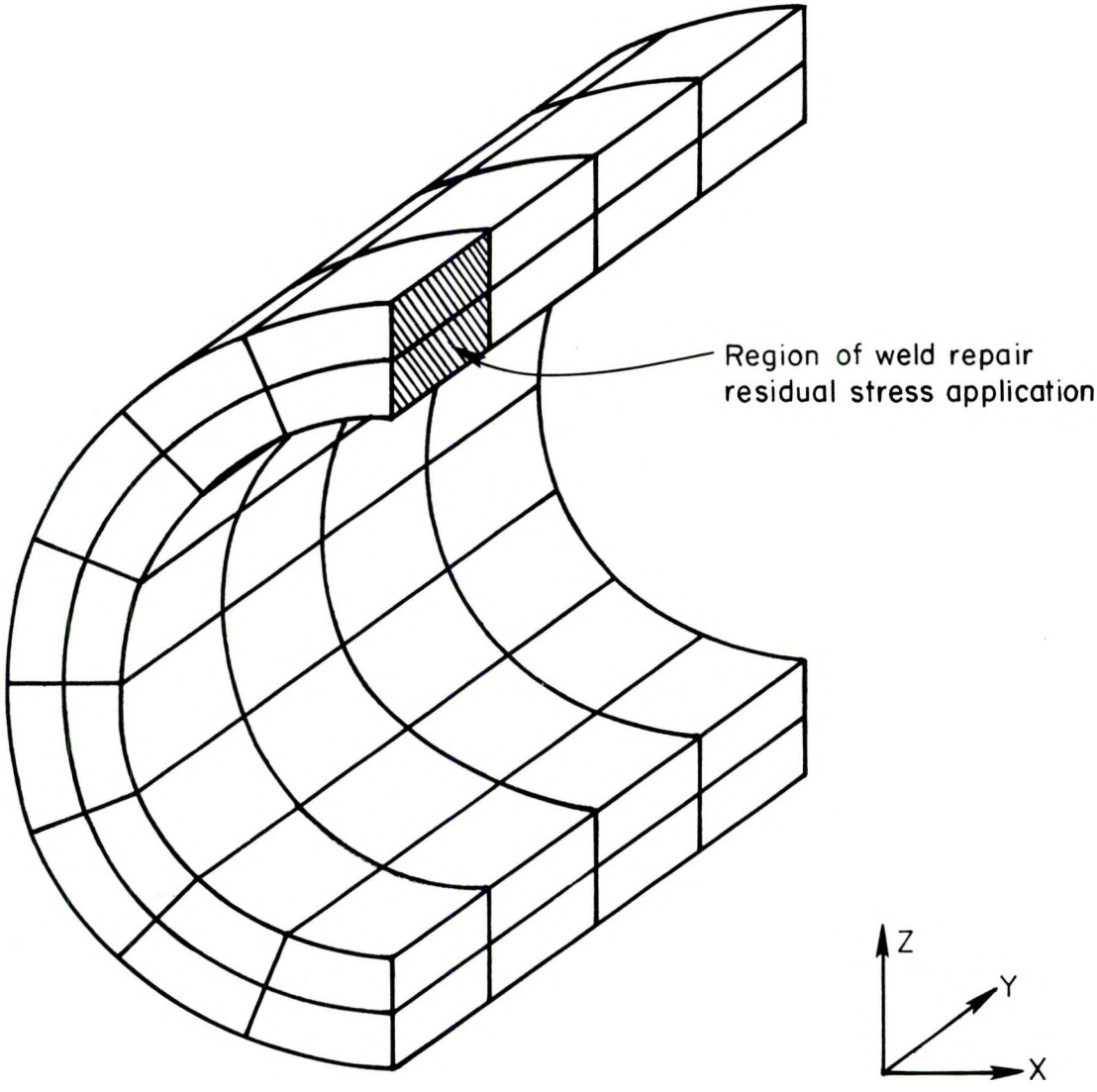

FIGURE 3. FINITE ELEMENT GRID FOR THREE-DIMENSIONAL STIFFNESS EFFECTS OF WELD REPAIR REGION.

The differences in stiffness due to the plane strain constraint for the two load types are shown in Table 1.

In order to establish the required stiffness of the coupling springs, an iterative approach was used in which the spring stiffness was varied in order to match both the stiffness and the stress state obtained in the 3D analysis. In order to keep the coupling stiffness independent of the grid spacing, it was necessary that the individual spring stiffnesses be adjusted depending on the density of the nodes. To accomplish this, the coupling stiffness was specified per unit area, i.e. in lb/in./in.^{2}. In determining the stiffness, both load cases were studied since the thermal induced stresses would contain both types of loading.

Some of the solutions obtained in the iteration process are included in Figures 4 and 5. Figure 4 contains the dependence of the outer surface σ_x stress (see Figure 3 for direction) on the angular position for the uniform stress load case. Results for two types of spring couplings are shown in Figure 4. The 3D model results are plotted and have a curve fitted through them. The addition of the plane strain constraint to the 3D solution had negligible effects on this distribution. During this process, it was found that it was difficult to match the shape of the 3D curve if the coupling stiffness was maintained constant for all angular positions. The reason for this is believed to be that the coupling adjacent to the free surface at the weld repair cavity must be zero in the direction normal to the free surface. Therefore, the coupling stiffness was input so that it was zero at the free surface, increased linearly to a given angle θ^* and then maintained constant. Figure 4a shows the results with constant coupling stiffness and Figure 4b shows the results with the improved method which uses a varying stiffness. In general, it would be expected that θ^* would be dependent on the axial length of the weld repair.

As mentioned previously, in addition to matching the stress state, it is also desirable to match the stiffness of the 3D solution. Table 1 contains the comparisons of the two types of 3D solutions and the 2D solutions contained in Figures 4 and 5. From Figure 4b it can be seen that the case of $K/A = 2.5 \times 10^6$ lb/in./in.^{2} and $\theta^* = 6.6$ degrees yields a stress state very nearly like the 3D solution. From Table 1 it can be seen that this selection matched the stiffness for this loading to within 5 percent.

Figure 5 contains σ_x stress distributions for the bending load case. Again, as evidenced by the one curve with θ^* equal to zero, there seems to be

TABLE 1. ANALYSIS DESCRIPTION FOR STUDY ON 3D EFFECTS ON THE STIFFNESS OF A WELD REPAIR CAVITY

Uniform Stress			Stiffness	3D comparison
Dimension	$K/A(\times 10^{-6})$	θ^* (deg)	$\frac{\sigma}{\delta}$ ($lb/in^2/in \times 10^{-6}$)	(%)
3	--	--	4.41	0†
3	(plane strain reinforced)		5.28	20
2	0.1	0.0	0.93	-79
2	0.6	0.0	3.09	-30
2	1.2	0.0	4.45	1
2	1.2	13.2	2.69	-39
2	2.0	8.8	3.58	-19
2	2.5	6.6	4.18	- 5
Bending Stress				
3	--	--	3.12	0†
3	(plane strain reinforced)		3.26	4
2	1.0	0.0	2.80	-10
2	1.5	6.6	2.13	-32
2	2.5	6.6	2.45	-21

† All comparisons based on the three-dimensional solutions

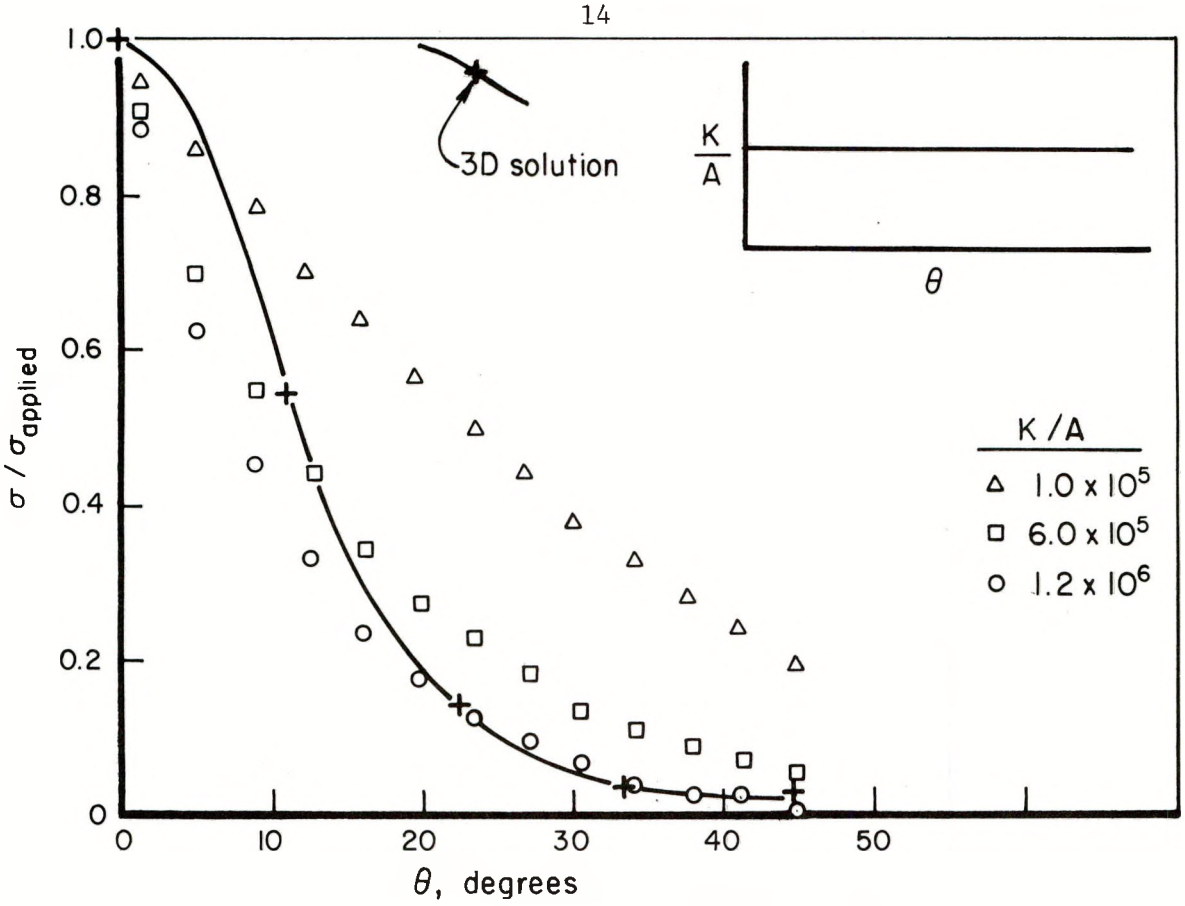

a. Constant Coupling Stiffness, K/A

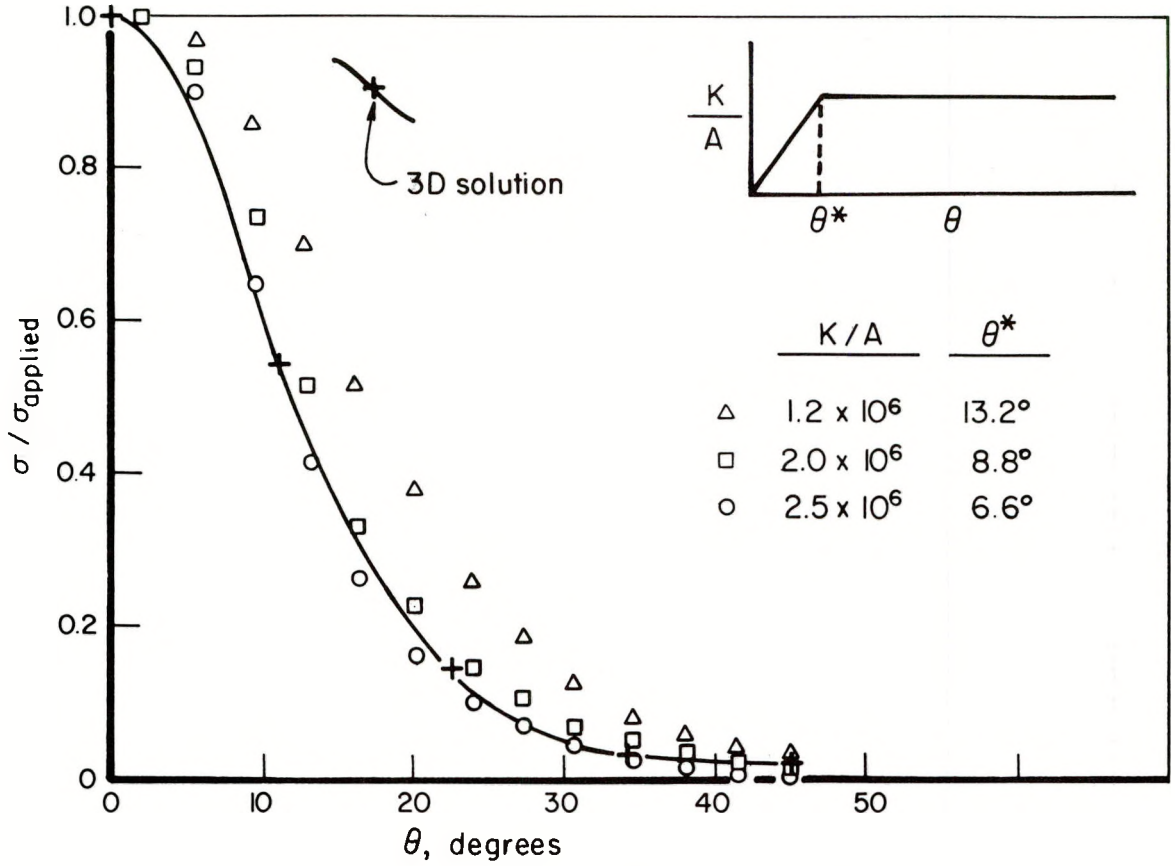

b. Variable Coupling Stiffness, K/A

FIGURE 4. COMPARISON OF STRESS STATES FOR THE 2D MODEL WITH 3D STIFFNESS EFFECTS FOR A UNIFORM APPLIED STRESS

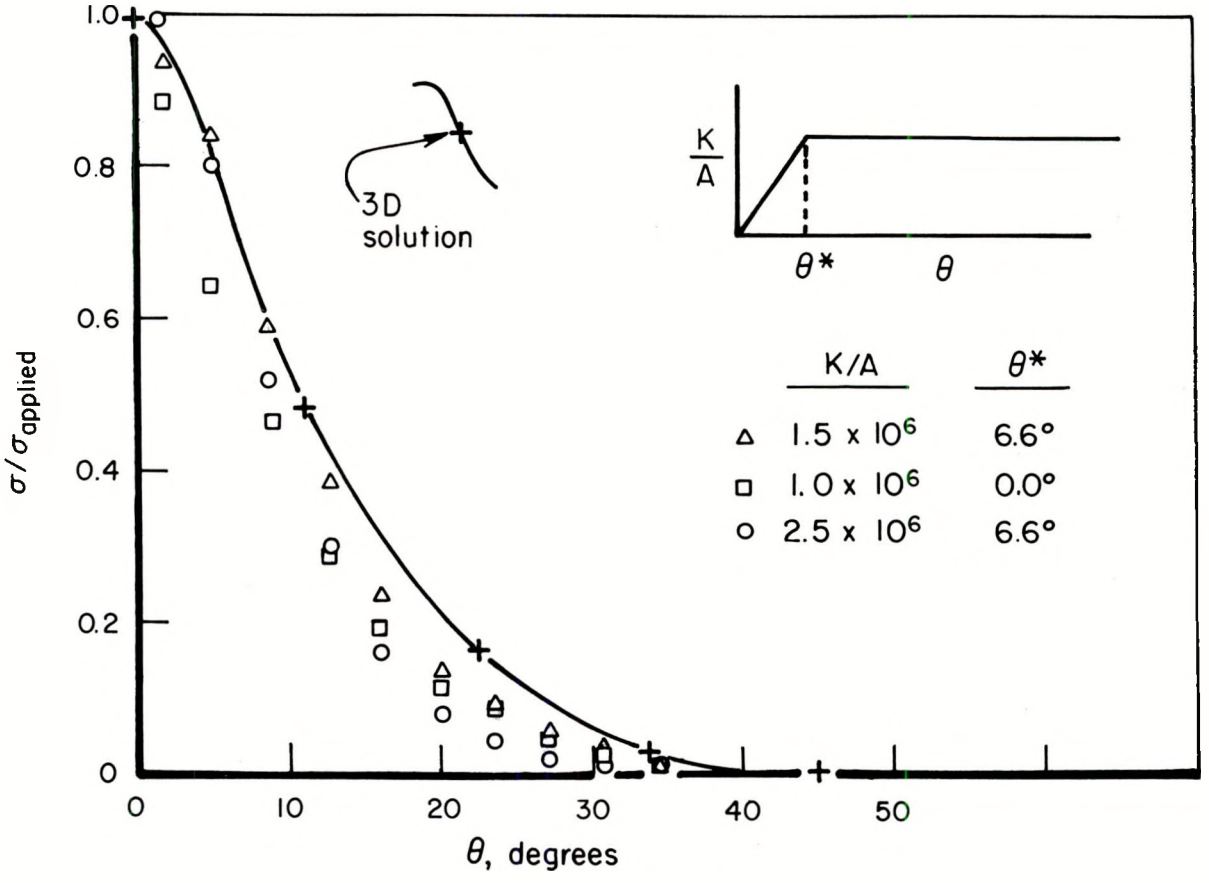

FIGURE 5. COMPARISON OF STRESS STATES FOR THE 2D MODEL WITH 3D STIFFNESS EFFECTS FOR AN APPLIED BENDING STRESS

better agreement with the 3D distribution if the coupling stiffness is made zero at the free surface. The bending load case was somewhat different from the uniform load case in the manner that the 2D model approximated the 3D behavior. In the uniform load case, it was possible to match both the overall stiffness as well as the stress distribution. In the bending load case, however, when the stress state was matched, the 2D model was more flexible than the 3D model. Thus, while the stiffness was matched, the stress states did not match (σ_x decayed too rapidly). However, the stiffness and value of θ^* which gave good agreement between the stiffness and the stress state for the uniform stress load case seemed to be those which gave the best compromise between stiffness and stresses for the bending load case. Table 1 shows that the overall stiffness for the solution using $K/A = 2.5 \times 10^6$ lb/in./in.^{2} and $\theta^* = 6.6$ degrees was underestimated by 21 percent while the stress state agreed to within 20 percent for circumferential distances of up to 4 inches. Trying to improve either of these values, was found to cause the other to suffer.

Based on this study, it appears that selecting this coupling method will produce a more realistic structural response than the simple assumption of plane strain. Because the thermal induced stress state will be a combination of the uniform and bending load cases, it is expected that the structural response will be at least as good as was found for the bending load case.

Plane Strain Formulation

This section contains a brief description of the changes required for an elastic-plastic thermal stress analysis under the conditions of plane strain ($\varepsilon_z = \tau_{xz} = \tau_{yz} = \gamma_{xz} = \gamma_{yz} = 0$). For the case of plane strain in an isotropic elastic material, the stresses are related to the strains in the following way

$$\begin{Bmatrix} \sigma_x \\ \sigma_y \\ \tau_{xy} \end{Bmatrix} = \frac{E}{1+\nu} \begin{bmatrix} \frac{1-\nu}{1-2\nu} & \frac{\nu}{1-2\nu} & 0 \\ & \frac{1-\nu}{1-2\nu} & 0 \\ \text{SYM} & & 1/2 \end{bmatrix} \begin{Bmatrix} \varepsilon_x - \alpha\Delta T \\ \varepsilon_y - \alpha\Delta T \\ \gamma_{xy} \end{Bmatrix} \qquad (2)$$

and $\sigma_z = \frac{\nu E}{(1+\nu)(1-2\nu)}(\varepsilon_x + \varepsilon_y - 2\alpha\Delta T)$

For an incremental elastic-plastic analysis, the stress-strain relations are in terms of incremental stresses and incremental strains. For the case of isotropic elastic-plastic material behavior, the relation between the incremental stresses and strains is derived through the use of the Prandtl-Reuss equations and takes the following form.

$$
\begin{aligned}
d(\varepsilon_x-\alpha\Delta T) &= \sigma'_x\, d\lambda + d(\sigma_x-\nu\sigma_y-\nu\sigma_z)/E \\
d(\varepsilon_y-\alpha\Delta T) &= \sigma'_y\, d\lambda + d(\sigma_y-\nu\sigma_z-\nu\sigma_x)/E \\
d(\varepsilon_z-\alpha\Delta T) &= \sigma'_z\, d\lambda + d(\sigma_z-\nu\sigma_x-\nu\sigma_y)/E \\
d\gamma_{xy} &= 2\,\tau_{xy}\, d\lambda + d\tau_{xy}/G \\
d\gamma_{yz} &= 2\,\tau_{yz}\, d\lambda + d\tau_{yz}/G \\
d\gamma_{zx} &= 2\,\tau_{zx}\, d\lambda + d\tau_{zx}/G
\end{aligned}
\qquad (3)
$$

where, $d\lambda = \frac{3}{2}\frac{d\bar{\sigma}}{\bar{\sigma}H}$; $H = \frac{d\bar{\sigma}}{d\varepsilon^p}$ (a material property) and σ'_x, σ'_y, σ'_z are the deviatoric stress components. Inverting Equation (3) to obtain incremental stresses in terms of the incremental strains and imposing the plane strain conditions, we have:

$$
\begin{Bmatrix} d\sigma_x \\ d\sigma_y \\ d\tau_{xy} \end{Bmatrix} = \frac{E}{1+\nu}
\begin{bmatrix}
\frac{1-\nu}{1-2\nu} - \frac{\sigma'^2_x}{S} & \frac{\nu}{1-2\nu} - \frac{\sigma'_x\sigma'_y}{S} & -\frac{\sigma'_x\tau_{xy}}{S} \\
 & \frac{1-\nu}{1-2\nu} - \frac{\sigma'^2_y}{S} & -\frac{\sigma'_y\tau_{xy}}{S} \\
\text{SYM} & & \frac{1}{2} - \frac{\tau^2_{xy}}{S}
\end{bmatrix}
\begin{Bmatrix} d(\varepsilon_x-\alpha\Delta T) \\ d(\varepsilon_y-\alpha\Delta T) \\ d\gamma_{xy} \end{Bmatrix} \qquad (4)
$$

and $d\sigma_z = \frac{E}{1+\nu}\left[\left(\frac{\nu}{1-2\nu} - \frac{\sigma'_x\sigma'_z}{S}\right) d(\varepsilon_x-\alpha\Delta T) + \left(\frac{\nu}{1-2\nu} - \frac{\sigma'_y\sigma'_z}{S}\right) d(\varepsilon_y-\alpha\Delta T) - \left(\frac{\sigma'_z\tau_{xy}}{S}\right) d\gamma_{xy}\right]$

where $S = \frac{2}{3}\bar{\sigma}^2\left(1+\frac{H}{3G}\right)$

In order to include the effect of thermal expansion in the constrained z-direction, it is necessary to modify the calculation of the thermal load vector. Ordinarily, the thermal contribution to the incremental load vector is calculated by:

$$\{df\}_{th} = \int_{Vol} [B]^T \{dT\} dV \tag{5}$$

where [B] is an elememt geometry dependent matrix relating element strains, $\{\varepsilon\}$, to the element nodal displacements $\{u\}$; and $\{dT\}$ is a vector of pseudo stresses given by

$$\begin{Bmatrix} dT_x \\ dT_y \\ dT_{xy} \end{Bmatrix} = \begin{bmatrix} \text{matrix from} \\ \text{Equation (4)} \\ \end{bmatrix} \begin{Bmatrix} \alpha\Delta T \\ \alpha\Delta T \\ 0 \end{Bmatrix} \tag{6}$$

For the case of plane strain, the thermal strain vector in Equation (6) must be replaced by:

$$\begin{Bmatrix} (1 + \nu_{eff})\ \alpha\Delta T \\ (1 + \nu_{eff})\ \alpha\Delta T \\ 0 \end{Bmatrix} , \tag{7}$$

where for elastic behavior $\nu_{eff} = \nu$, and for elastic-plastic behavior,

$$\nu_{eff} = \frac{3\nu(1+\frac{H}{3G}) + (1-2\nu)}{3(1+\frac{H}{3G}) - (1-2\nu)} . \tag{8}$$

Note that unlike the linear elastic case described by Equation (2), the elastic-plastic case contains the current stresses in Equation (4). In the analysis, the stress state at the beginning of the increment is used. Note that except for these equations, the analysis proceeds in the same way as that for plane stress. The plane strain capability for thermal elastic-plastic stress analysis was included in the analysis and checked for several test cases.

Simplified Stress Model and the Half Bead Technique

During this quarter, a study was also undertaken to determine the effect of the half-bead grinding technique on residual stresses. For this study, a simplified model was developed. The thermal analysis used the equation for a half space discussed previously. The stress analysis assumed perfectly constrained conditions in the plane parallel to the surface and plane stress condition in the thickness direction. The geometry is shown in Figure 6. Under these assumptions, the stress history at any layer is only a function of the temperature history of that layer and is not affected by the temperature and stress of neighboring layers. This set of assumptions is equivalent to placing successive layers of weld metal in a perfectly rigid repair cavity.

The mechanical properties of A533B were input as a function of temperature. The stress-strain curve was represented by three linear segments (an elastic segment, a work-hardening segment, and an ideally plastic segment). Elastic unloading was incorporated, but no Bauschinger effects were included. The response of the material was assumed to be time independent (i.e., no creep behavior was modeled). However, stress states were adjusted so as to include the effect of decreasing stress-strain properties with increasing temperature. If the temperature exceeded 2100F (1150C), the reference temperature was taken as 2100F and stresses were set to zero. Otherwise, the ambient temperature of 450F (230C) was used. The input parameters to the thermal model were those for a 3/32-inch weld rod (90 amps, 23 volts, 7.5 in/min.). Each pass was assumed to have a height of 0.07 inch.

The output of the analysis contained both temperature and stress histories. The temperature history consists of the maximum temperature reached during each pass application as shown in Figure 7. The location considered in this Figure is 0.28 inch below the initial surface of the weld cavity. The results in Figure 7 show that the maximum temperature decayed rapidly with increasing number of passes and approached asymptotically the ambient temperature. The maximum temperature was determined by solving a transcendental equation using the secant method.

The stress results obtained from this simple model show that at this depth stresses oscillate beyond elastic limits in compression and then tension for each pass through pass 5 (Figure 8). For passes 1 through 5, the compressive stresses at the peak temperatures increase because of the increase in

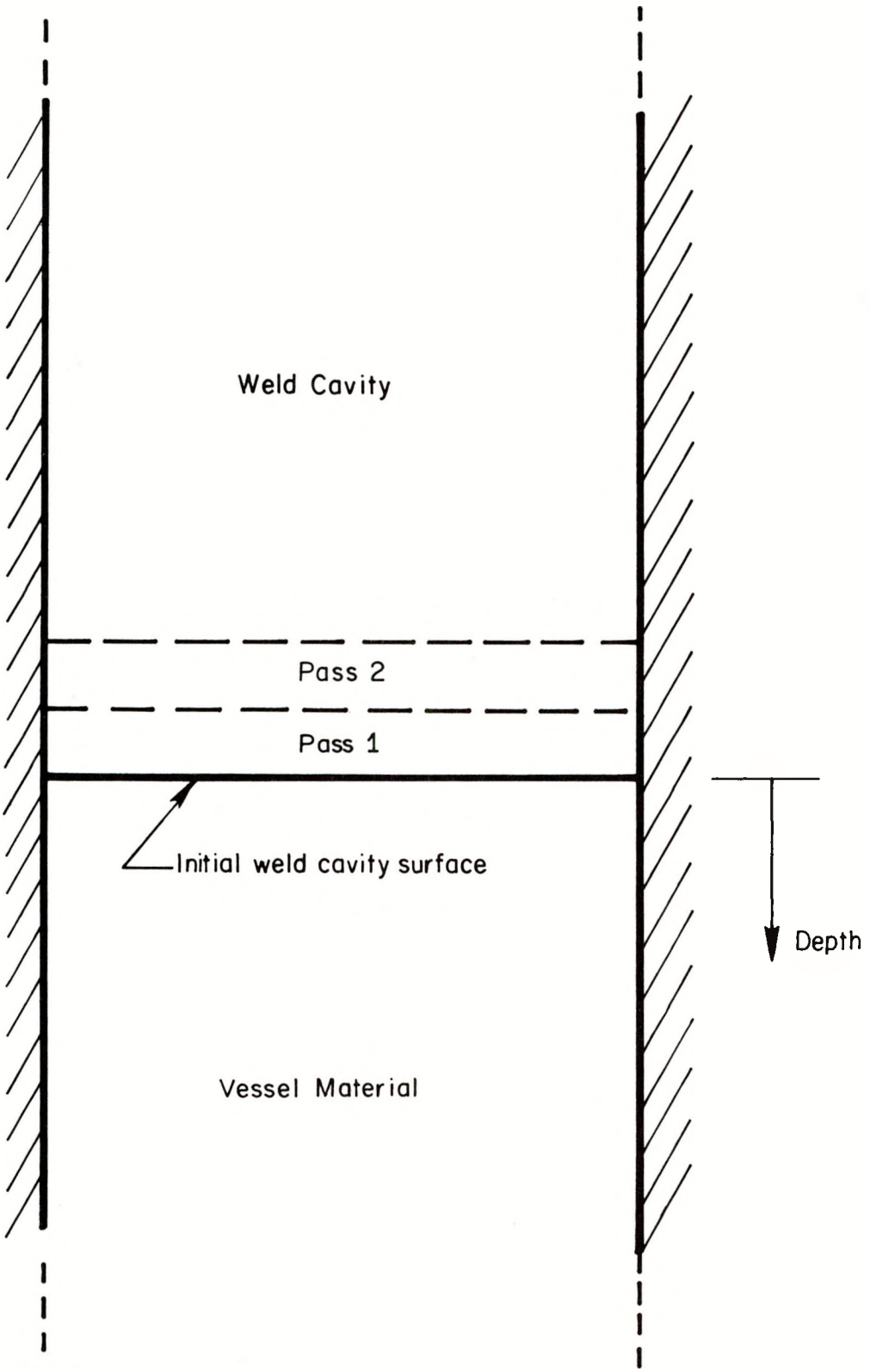

FIGURE 6. SIMPLIFIED MODEL FOR HALF-BEAD GRINDING STUDY

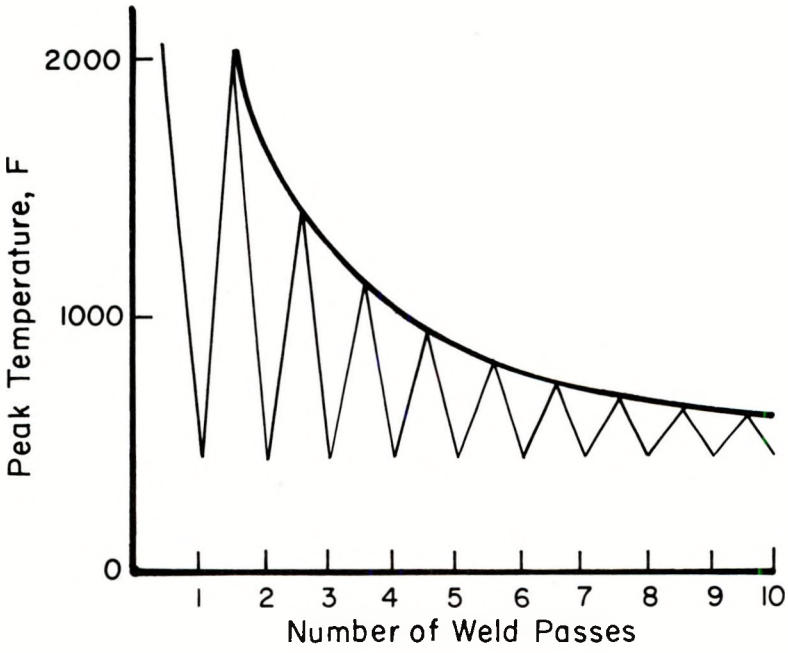

FIGURE 7. TEMPERATURE RANGES CALCULATED BY THE THERMAL MODEL AND USED AS INPUT TO THE SIMPLIFIED STRESS MODEL

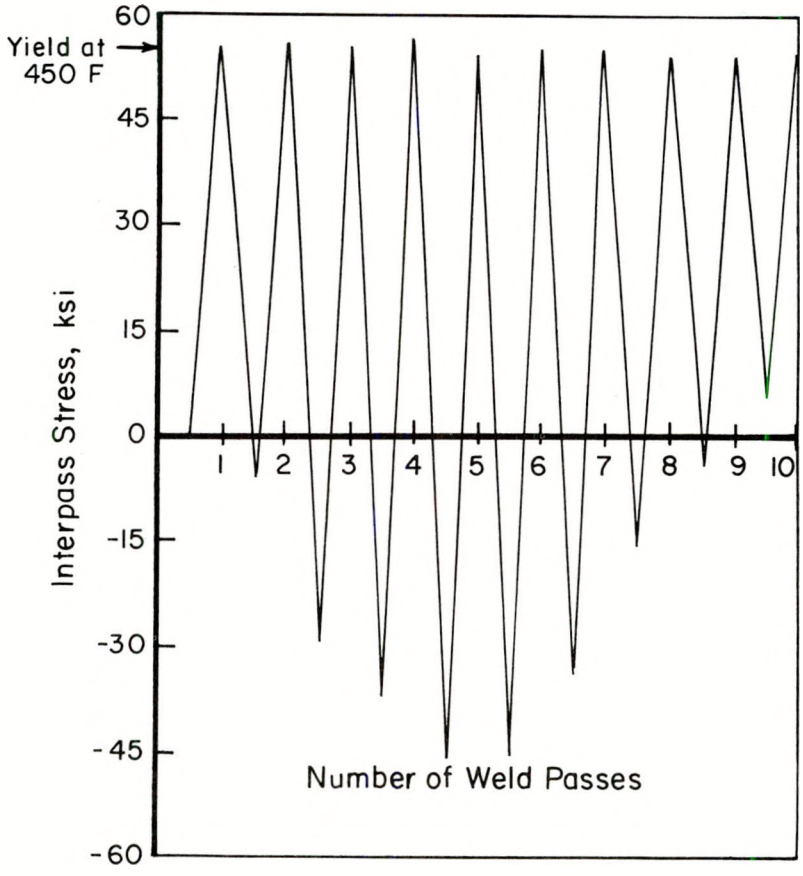

FIGURE 8. STRESS RANGES CALCULATED BY THE SIMPLIFIED STRESS MODEL

strength at the successively lower temperatures. For each pass subsequent to pass 6, the compressive stress decreases and finally goes tensile because the temperature excursions have lessened to the point that the stresses are varying elastically.

Figure 9 shows the maximum temperature and final residual stress at various depths below the initial weld cavity surface. The maximum temperature corresponds to the temperature reached during the first pass, since for this pass, the heat source was nearer than for all the following passes. The residual stresses correspond to those after ten passes. However, as suggested by Figure 8, the residual stresses after the first pass differed from this distribution by less than 1 ksi. Therefore, in this simplified model, the residual stress at any depth only depends on the maximum temperature excursion experienced at that depth. Also, since all the material in the weld passes will have reference temperatures of 2100F, these weld passes will behave exactly as the vessel material which was located at depths of less than 0.4 inch.

In addition to the temperature level of 2100F which was somewhat arbitrarily chosen as the limit above which stresses are negligible, two other temperature levels appear to have significance in this analysis. In Figure 9, it can be seen that for all material at a depth of less than 1.0 inch, the final residual stress had the same value of 53 ksi. In terms of maximum temperatures, this represents a temperature excursion of at least 350 degrees from the ambient temperature of 450F. At depths with excursions between 150 and 350 degrees, the residual stress is in the elastic range. At depths with excursions less than 150 degrees, the residual stress is essentially zero.

Based on the results obtained from this simplified model, some insight into the effect of the half-bead grinding technique on the final residual stresses is possible. It appears that grinding of the initial layer of welds and the resulting shift by one half bead height of all remaining passes has a negligible effect on the final residual stresses. This is due to two factors. The first is that each weld pass layer application wipes out any previous stress history up to a depth of 0.4 inch. This is because the strength up to this depth is reduced to negligible levels by temperatures exceeding 2100F (see Figure 9). The second effect is that all material exceeding 800F will experience sufficient plasticity to wipe out any previous stress history and will end up with stresses on the order of the material yield at 450F. Since the maximum temperatures at

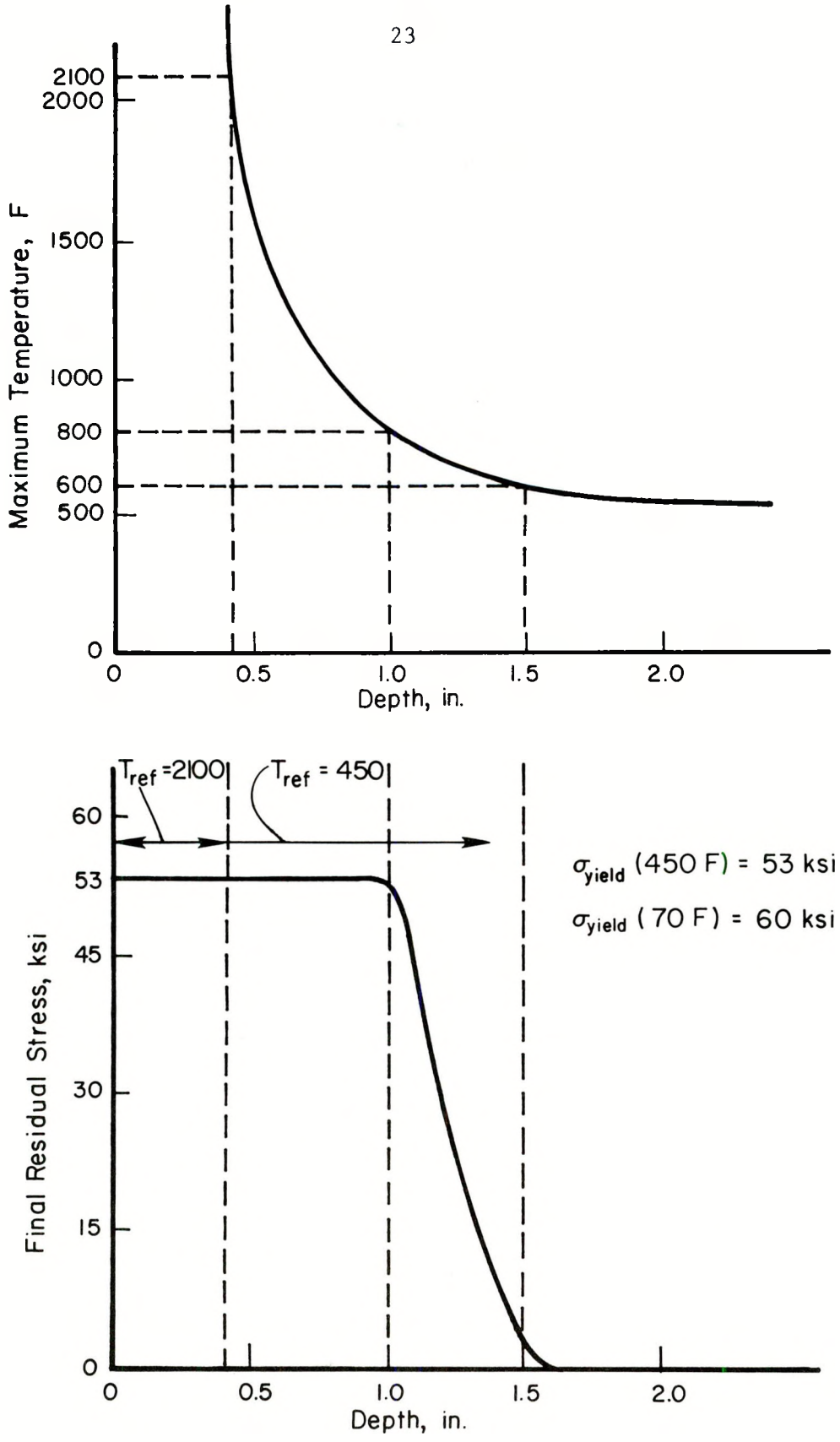

FIGURE 9. MAXIMUM TEMPERATURES AND FINAL RESIDUAL STRESSES PREDICTED BY THE SIMPLIFIED STRESS MODEL

any point below the weld material will occur for the first pass (due to the heat source being shifted further away for each subsequent pass by either one half or a whole bead height), the final stresses will also be determined by this pass.

IV. RELATED ACTIVITIES

In addition to the research activities described in preceding sections, efforts have been devoted to disseminating the technical results. This is done through presentations at public information meetings and technical society meetings. During the first quarter, a presentation was made at the Fifth Water Reactor Technology Meeting, held November 7-8, 1977, at the National Bureau of Standards in Gaithersburg, Maryland. A Research Information Letter was written and distributed at this meeting.

Technical papers were also prepared for the American Society of Mechanical Engineer's Winter Annual Meeting held November 28 - December 2, 1977 in Atlanta, Georgia and the ASME June meeting in Montreal.

A visit to Oak Ridge National Laboratories (ORNL) was made on October 12, 1977 for the purpose of discussing residual stress data obtained for the Heavy Section Steel Technology program. The data will be used to verify the residual stress analysis program. Discussions with people working on the HSST program at ORNL were continued following this meeting via telephone conversations.

V. PLANS FOR NEXT QUARTER

Plans for the Second Quarter include a sensitivity study with the temperature model and further development of the residual stress analysis model. The temperature analysis model will be used in a sensitivity study to evaluate the effect of changes in the weld parameters on the temperature distributions that are used in the residual stress analysis. Development of the residual stress analysis model will continue during the second quarter with an investigation of iteration techniques to better represent the nonlinearities and to handle the large number of passes in the weld repair. To date, the focus of this work has been on residual stresses on the inside and outside surfaces of the pipes and vessels. Plans for next quarter include an examination of the residual stress distributions through the thickness. An updated analysis of the weld repair of the HSST ITV-8 is planned using the three-dimensional stiffness effects developed during the first quarter.

REFERENCES

[1] Rybicki, E. F., et.al., "Residual Stresses at Girth-Butt Welds in Pipes and Pressure Vessels", Final Report to U.S. Nuclear Regulatory Commission Division of Reactor Safety Research under Contract No. AT (49-24)-0293, NUREG-0376, published November 1977.

[2] ASME Boiler and Pressure Vessel Code, Section XI, Rules for In-Service Inspection of Nuclear Power Plant Components.

[3] Smith, G. C., "Residual Stress Measurements on a Thick-Walled Cylinder With an ASME Section XI Weld Repari" in Heavy-Section Steel Technology Program Quarterly Progress Report for October - December 1976, by G. Whitman, ORNL/NUREG/TM-94, published April, 1977.

☆ U. S. GOVERNMENT PRINTING OFFICE : 1978—720-387/68

UNITED STATES
NUCLEAR REGULATORY COMMISSION
WASHINGTON, D. C. 20555

OFFICIAL BUSINESS
PENALTY FOR PRIVATE USE, $300

POSTAGE AND FEES PAID
U.S. NUCLEAR REGULATORY
COMMISSION